Geomechanics and Engineering, *Vol. 33, No. 5 (2023) 427-437*
https://doi.org/10.12989/gae.2023.33.5.427

Wave propagation of FGM plate via new integral inverse cotangential shear model with temperature-dependent material properties

Mokhtar Ellali[1], Mokhtar Bouazza*[2,4] and Ashraf M. Zenkour[3,5]

[1]*Smart Structures Laboratory, University of Ain Témouchent-Belhadj Bouchaib,46000,Algeria*
[2]*Department of Civil Engineering, University Tahri Mohamed of Bechar, Bechar 08000, Algeria*
[3]*Department of Mathematics, Faculty of Science, King Abdulaziz University, P.O. Box 80203, Jeddah 21589, Saudi Arabia*
[4]*Laboratory of Materials and Hydrology (LMH), University of Sidi Bel Abbes, Sidi Bel Abbes 22000, Algeria*
[5]*Department of Mathematics, Faculty of Science, Kafrelsheikh University, Kafrelsheikh 33516, Egypt*

(*Received July 25, 2022, Revised February 24, 2023, Accepted March 7, 2023*)

Abstract. The objective of this work is to study the wave propagation of an FGM plate via a new integral inverse shear model with temperature-dependent material properties. In this contribution, a new model based on a high-order theory field of displacement is included by introducing indeterminate integral variables and inverse co-tangential functions for the presentation of shear stress. The temperature-dependent properties of the FGM plate are assumed mixture of metal and ceramic, and its properties change by the power functions of the thickness of the plate. By applying Hamilton's principle, general formulas of wave propagation were obtained to plot the phase velocity curves and wave modes of the FGM plate with simply supported edges. The effects of the temperature and volume fraction by distributions on wave propagation of the FGM plate are investigated in detail. The results of the dispersion and the phase velocity curves of the propagation wave in the functionally graded plate are compared with previous research.

Keywords: FGM plate; new integral inverse shear model; temperature-dependent material properties; wave propagation

1. Introduction

Although composite structures have extensively been utilized in many applications ranging from aerospace to common facilities, the main concern has always been the optimization of such structures, especially for hi-tech engineering applications. Achievement of the most compact/economic component that meets all the relevant design criteria necessitates employing more accurate modeling procedures and accurate theories in the design stage. Some plate-type composite structures are vulnerable to severe temperatures or thermal gradients induced by the environment. In certain cases, the thermal load turns out to be the primary load, and the thermal stability of the composite is one of the factors governing their design (Ashour 2003, Ellali *et al.* 2018, Bouazza *et al.* 2019, Grover *et al.* 2013).

Many publications have appeared in the literature on the free and forced vibration of shear deformable composite plates. The free vibration of transversely isotropic magneto-electro-elastic laminated circular plates was analyzed by Chen *et al*. (2006). To present accurate mechanical behavior analysis of plates and shells, different theoretical models have been developed. Recently, the nonlinear flexural analysis of laminated composite flat panels under hygro-thermo-mechanical loading was presented by Kar *et al.* (2015) based on various higher-order shear deformation plate theories. The material properties of the composite are affected by the variation of temperature and moisture and are based on a micro-mechanical model of laminates. Bouazza *et al.* (2016) developed an analytical solution of refined hyperbolic shear deformation theory to obtain the critical buckling temperature of cross-ply laminated plates with a simply supported edge. Bouazza and Benseddiq (2015) investigated analytical modeling for the thermoelastic buckling behavior of functionally graded rectangular plates (FGM) under thermal loadings. Buckling of symmetrically laminated plates using nth-order shear deformation theory with curvature effects was studied by Becheri *et al.* (2016). The effect of temperature on the interface stresses of composite plate beams is presented by Bouazza *et al.* (2019). Bouderba *et al.* (2013) studied the thermo-mechanical bending response of FGM plates resting on elastic foundations. A nonlocal zeroth-order shear deformation plate theory was introduced for free vibration analysis of functionally graded nanoscale plates resting on an elastic foundation by Bounouara *et al.* (2016). To overcome the limitations of traditional methods, in recent years novel and modified methods have been proposed for the investigation of buckling and wave propagation flexural behavior of the composite plates by example (Dehshahri *et al.* 2015, Mellouli *et al.* 2019, Nazira *et al.* 2019, Ebrahimi *et al.* 2019, Bensattalah *et al.* 2019, Kahya *et al.* 2019). Recently, several novels and modified theories have been developed for the behavior analysis of composites and wave

*Corresponding author, Professor
E-mail: bouazza_mokhtar@yahoo.fr
bouazza.mokhtar@univ-bechar.dz

ISSN: 2005-307X (Print), 2092-6219 (Online)

propagation in FGM structures (Ebrahimi and Dabbagh 2018, Ebrahimi *et al.* 2021a, b, c 2022a, Daikh *et al.* 2021, Alazwari *et al.* 2022, Basha *et al.* 2022, Soliman *et al.* 2018, Melaibari *et al.* 2022, Bashiri *et al.* 2021, Sahoo *et al.* 2022, Hissaria *et al.* 2022, Bouazza and Zenkour 2020, Choudhary *et al.* 2022, Ramteke *et al.* 2022a, b, Yang *et al.* 2020, Zheng *et al.* 2018, Pham *et al.* 2022, Tho *et al.* 2023, Garg *et al.* 2023, Zenkour and El-Shahrany 2022).

The wave propagation characteristics of FGM plates with temperature-dependent material properties are investigated via a new integral inverse shear model. This theory does not use shear correction factors. The temperature field is assumed to be constant in the plane and only varies in the thickness of the plate. Material properties are assumed to be temperature-dependent and graded in the thickness direction according to a simple power-law distribution in terms of the volume fractions of the constituents. The paper introduced a new mathematical model to analyze the graded structure under a thermal environment based on a high-order theory field of displacement is included by introducing indeterminate integral variables and inverse co-tangential function for the presentation of shear stress. The governing equations of the wave propagation are obtained for the FGM plate for simply-supported boundary conditions by using Hamilton's principle. The dispersion phase velocity and mode curves of the wave propagation in the functionally graded plate in thermal environments are plotted. The influences of the volume fraction index and temperature on the dispersion phase velocity and mode of the wave propagation in the functionally graded plate are also clearly discussed.

2. Theoretical formulation

The properties of FGM plates are expressed by the law of mixing as follows (Shen *et al*. 2009, Bui *et al*. 2016)

$$P = P_t V_c + P_b V_m, \tag{1}$$

with P_b and P_t the properties of metal and ceramic respectively and can be given as a function of the temperature variation (Shen *et al.* 2009, Bui *et al.* 2016)

$$P = P_0(P_{-1}T^{-1} + 1 + P_1 T + P_2 T^2 + P_3 T^3), \tag{2}$$

where P_0, P_{-1}, P_1, P_2 and P_3 are the coefficients showing the temperature - the dependence of the properties of the material. T(K) is the ambient temperature. It is assumed that Young's modulus, coefficient of thermal expansion α, and Poisson's ratio ν of the FGM plate are dependent on temperature, while density ρ and thermal conductivity λ are independent of temperature (Sun and Luo 2011)

$$\begin{aligned} E(z,T) &= [E_t(T) - E_b(T)]\left(\frac{2z+h}{2h}\right)^N + E_b(T), \\ \alpha(z,T) &= [\alpha_t(T) - \alpha_b(T)]\left(\frac{2z+h}{2h}\right)^N + \alpha_b(T), \\ \nu(z,T) &= [\nu_t(T) - \nu_b(T)]\left(\frac{2z+h}{2h}\right)^N + \nu_b(T), \end{aligned} \tag{3}$$

$$\rho(z) = [\rho_t - \rho_b]\left(\frac{2z+h}{2h}\right)^N + \rho_b,$$

$$\lambda(z) = [\lambda_t - \lambda_b]\left(\frac{2z+h}{2h}\right)^N + \lambda_b.$$

The volume fraction of ceramic would vary through the thickness in the form of power-law (P-FGM)

$$V_c = \left(\frac{2z+h}{2h}\right)^N, \tag{4}$$

where N is the parameter of the material which is greater than or equal to zero. The volume fractions are related to each other as

$$V_c + V_m = 1. \tag{5}$$

In this work, one considers that the variation of temperature of this product in the thickness is supposed to be one-dimensional is constant in the x-y plane of the plate. This equation is given by the heat transfer equation of state by the following expression (Bouazza and Benseddiq 2015)

$$-\frac{\mathrm{d}}{\mathrm{d}z}\left[\lambda(z)\frac{\mathrm{d}T}{\mathrm{d}z}\right] = 0 \tag{6}$$

We consider the boundary conditions

$$\begin{aligned} z = h/2 \quad \text{at} \quad T = T_t \\ z = -h/2 \quad \text{at} \quad T = T_b. \end{aligned} \tag{7}$$

To solve this equation using the polynomial series is obtained as follows

$$T(z) = T_b + (T_t - T_b)\eta(z), \tag{8}$$

where

$$\begin{aligned} \eta(z) = \frac{1}{\vartheta}\Bigg[\left(\frac{2z+h}{2h}\right) - \frac{\lambda_{tb}}{(N+1)\lambda_b}\left(\frac{2z+h}{2h}\right)^{N+1} + \\ \frac{\lambda_{tb}^2}{(2N+1)\lambda_b^2}\left(\frac{2z+h}{2h}\right)^{2N+1} - \frac{\lambda_{tb}^3}{(3N+1)\lambda_b^3}\left(\frac{2z+h}{2h}\right)^{3N+1} \\ + \frac{\lambda_{tb}^4}{(4N+1)\lambda_b^4}\left(\frac{2z+h}{2h}\right)^{4N+1} - \frac{\lambda_{tb}^5}{(5N+1)\lambda_b^5}\left(\frac{2z+h}{2h}\right)^{5N+1}\Bigg], \end{aligned} \tag{9}$$

and

$$\begin{aligned} \vartheta = 1 - \frac{\lambda_{tb}}{(N+1)\lambda_b} + \frac{\lambda_{tb}^2}{(2N+1)\lambda_b^2} - \frac{\lambda_{tb}^3}{(3N+1)\lambda_b^3} \\ + \frac{\lambda_{tb}^4}{(4N+1)\lambda_b^4} - \frac{\lambda_{tb}^5}{(5N+1)\lambda_b^5} \end{aligned} \tag{10}$$

$$\lambda_{tb} = \lambda_t - \lambda_b.$$

The present approach is developed based on the assumptions of the inverse trigonometric shear strain theory in which the axial displacements contain an integral component that can be given as follows (Ellali *et al*. 2022)

$$\begin{aligned} u(x,y,z,t) &= u_0(x,y,t) - z\frac{\partial w_0}{\partial x} + S_1 f(z)\int \theta(x,y,t)\mathrm{d}x, \\ v(x,y,z,t) &= v_0(x,y,t) - z\frac{\partial w_0}{\partial y} + S_2 f(z)\int \theta(x,y,t)\mathrm{d}x, \\ w(x,y,z,t) &= w_0(x,y,t), \end{aligned} \tag{11}$$

where t denotes time, u_0, v_0, w_0 and θ are the four unknowns of the displacements of the mean surface of the plate, $f(z)$ presents the shape function which defines the distribution of transverse shear stresses and strains through the thickness of the plate. The constants S_1 and S_2 depend on the geometry. In this study, we take the function $f(z)$ as follows

$$f(z) = \cot^{-1}\left(\frac{rh}{z}\right) - z\frac{4r}{h(4r^2+1)}; \quad r = 0.46 \tag{12}$$

In the field of linear elasticity, the displacement-strain relation associated with the field of this approach is expressed in the following form

$$\begin{Bmatrix}\varepsilon_x\\ \varepsilon_y\\ \varepsilon_{xy}\end{Bmatrix} = \begin{Bmatrix}\varepsilon_x^0\\ \varepsilon_y^0\\ \gamma_{xy}^0\end{Bmatrix} + z\begin{Bmatrix}k_x^b\\ k_y^b\\ k_{xy}^b\end{Bmatrix} + f(z)\begin{Bmatrix}k_x^s\\ k_y^s\\ k_{xy}^s\end{Bmatrix},$$
$$\begin{Bmatrix}\gamma_{xz}\\ \gamma_{yz}\end{Bmatrix} = g(z)\begin{Bmatrix}\gamma_{xz}^0\\ \gamma_{yz}^0\end{Bmatrix}, \tag{13}$$

where

$$\begin{Bmatrix}\varepsilon_x^0\\ \varepsilon_y^0\\ \varepsilon_{xy}^0\end{Bmatrix} = \begin{Bmatrix}\dfrac{\partial u_0}{\partial x}\\ \dfrac{\partial v_0}{\partial y}\\ \dfrac{\partial u_0}{\partial y} + \dfrac{\partial v_0}{\partial x}\end{Bmatrix}, \quad \begin{Bmatrix}k_x^b\\ k_y^b\\ k_{xy}^b\end{Bmatrix} = \begin{Bmatrix}-\dfrac{\partial^2 w_0}{\partial x^2}\\ -\dfrac{\partial^2 w_0}{\partial y^2}\\ -2\dfrac{\partial^2 w_0}{\partial x \partial y}\end{Bmatrix},$$
$$\begin{Bmatrix}k_x^s\\ k_y^s\\ k_{xy}^s\end{Bmatrix} = \begin{Bmatrix}S_1\theta\\ S_2\theta\\ S_1\frac{\partial}{\partial y}\int\theta dx + S_2\frac{\partial}{\partial x}\int\theta dy\end{Bmatrix}, \quad \begin{Bmatrix}\gamma_{xz}^0\\ \gamma_{yz}^0\end{Bmatrix} = \begin{Bmatrix}S_1\int\theta dx\\ S_2\int\theta dy\end{Bmatrix}, \quad g(z) = \frac{\mathrm{d}f(z)}{\mathrm{d}z}. \tag{14}$$

The integral terms used in the displacement field equations can be solved using Navier's solution and can be given by

$$\int\theta\,\mathrm{d}x = A'\frac{\partial\theta}{\partial x}, \quad \int\theta\,\mathrm{d}y = B'\frac{\partial\theta}{\partial y},$$
$$\frac{\partial}{\partial y}\int\theta\,\mathrm{d}x = A'\frac{\partial^2\theta}{\partial x\partial y}, \quad \frac{\partial}{\partial x}\int\theta\,\mathrm{d}y = B'\frac{\partial^2\theta}{\partial x\partial y}. \tag{15}$$

According to the type of solution used, the coefficients A', B', k_1 and are chosen, in this contribution, Navier's solution is used. The coefficients A', B', k_1 and k_2 are given as follows

$$A' = -\frac{1}{k_1^2}, \quad B' = -\frac{1}{k_2^2},$$
$$S_1 = z, \quad S_2 = k_2^2. \tag{16}$$

The constitutive equations of the FGM plates of linear elasticity concerning the stresses to the strains taken into account of the thermal effects are given by (Kar *et al.* 2015)

$$\begin{Bmatrix}\sigma_x\\ \sigma_y\\ \sigma_{xy}\\ \tau_{yz}\\ \tau_{xz}\end{Bmatrix} = \begin{bmatrix}Q_{11} & Q_{12} & 0 & 0 & 0\\ Q_{21} & Q_{22} & 0 & 0 & 0\\ 0 & 0 & Q_{66} & 0 & 0\\ 0 & 0 & 0 & Q_{44} & 0\\ 0 & 0 & 0 & 0 & Q_{55}\end{bmatrix}\left(\begin{Bmatrix}\varepsilon_x\\ \varepsilon_y\\ \varepsilon_{xy}\\ \gamma_{yz}\\ \gamma_{xz}\end{Bmatrix} - \alpha T\begin{Bmatrix}1\\ 1\\ 0\\ 0\\ 0\end{Bmatrix}\right), \tag{17}$$

where

$$Q_{11} = Q_{22} = \frac{E(z,T)}{1-\nu(z,T)^2},$$
$$Q_{12} = Q_{21} = \frac{\nu(z,T)E(z,T)}{1-\nu(z,T)^2},$$
$$Q_{44} = Q_{55} = Q_{66} = \frac{E(z,T)}{2[1+\nu(z,T)]}, \tag{18}$$

where $\left(N_i, M_i^b, M_i^s\right)$ and $\left(S_{xz}^s, S_{yz}^s\right)$ are the resultants of the stresses in a plate FGM can be expressed by integrating Eq. (19) on the thickness. The resultants of stress are given by

$$\left(N_i, M_i^b, M_i^s\right) = \int_{-h/2}^{h/2}\sigma_i\left(1, z, f(z)\right)\mathrm{d}z, \quad i = x, y, xy,$$
$$\left(S_{xz}^s, S_{yz}^s\right) = \int_{-h/2}^{h/2} g(z)\left(\tau_{xz}, \tau_{yz}\right)\mathrm{d}z, \tag{19}$$
$$\left(N^T, M^{bT}\right) = \int_{-h/2}^{h/2}\alpha\Delta T\frac{E(z,T)}{1-\nu(z,T)}(1, z)\,\mathrm{d}z.$$

Replacing Eq. (17) in Eq. (19) gives Eq. (20), the resulting stresses from this proposed model can be obtained in terms of strains and stiffness elements as follows

$$\begin{Bmatrix}N\\ M^b\\ M^s\end{Bmatrix} = \begin{bmatrix}A & B & B^s\\ B & D & D^s\\ B^s & D^s & H^s\end{bmatrix}\begin{Bmatrix}\varepsilon\\ k^b\\ k^s\end{Bmatrix} - \begin{Bmatrix}N^T\\ M^{bT}\\ M^{sT}\end{Bmatrix}, \quad S = A^s\gamma \tag{20}$$

where

$$N = \left\{N_x, N_y, N_{xy}\right\}^t, \quad M^b = \left\{M_x^b, M_y^b, M_{xy}^b\right\}^t,$$
$$M^s = \left\{M_x^s, M_y^s, M_{xy}^s\right\}^t,$$
$$N^T = \left\{N_x^T, N_y^T, 0\right\}^t, \quad M^{bT} = \left\{M_x^{bT}, M_y^{bT}, 0\right\}^t,$$
$$M^{sT} = \left\{M_x^{sT}, M_y^{sT}, 0\right\}^t,$$
$$\varepsilon = \left\{\varepsilon_x^0, \varepsilon_y^0, \varepsilon_{xy}^0\right\}^t, \quad k^b = \left\{k_x^b, k_y^b, k_{xy}^b\right\}^t,$$
$$k^s = \left\{k_x^s, k_y^s, k_{xy}^s\right\}^t,$$
$$A = \begin{bmatrix}A_{11} & A_{12} & 0\\ A_{12} & A_{22} & 0\\ 0 & 0 & A_{66}\end{bmatrix}, \quad B = \begin{bmatrix}B_{11} & B_{12} & 0\\ B_{12} & B_{22} & 0\\ 0 & 0 & B_{66}\end{bmatrix},$$
$$B^s = \begin{bmatrix}B_{11}^s & B_{12}^s & 0\\ B_{12}^s & B_{22}^s & 0\\ 0 & 0 & B_{66}^s\end{bmatrix}, \quad D = \begin{bmatrix}D_{11} & D_{12} & 0\\ D_{12} & D_{22} & 0\\ 0 & 0 & D_{66}\end{bmatrix},$$
$$D^s = \begin{bmatrix}D_{11}^s & D_{12}^s & 0\\ D_{12}^s & D_{22}^s & 0\\ 0 & 0 & D_{66}^s\end{bmatrix}, H^s = \begin{bmatrix}H_{11}^s & H_{12}^s & 0\\ H_{12}^s & H_{22}^s & 0\\ 0 & 0 & H_{66}^s\end{bmatrix}, \tag{21}$$

and

$$S = \left\{S_{xz}^s, S_{yz}^s\right\}^t, \quad \gamma = \left\{\gamma_{xz}^0, \gamma_{yz}^0\right\}^t, \quad A^s = \begin{bmatrix}A_{44}^s & 0\\ 0 & A_{55}^s\end{bmatrix} \tag{22}$$

The stiffness rigidity terms of this model are defined as follows

$$\begin{aligned}&\{A_{ij}, B_{ij}, D_{ij}, B^s_{ij}, D^s_{ij}, H^s_{ij}\}\\&= \int_{-\frac{h}{2}}^{\frac{h}{2}} Q_{ij}\{1, z, z^2, f(z), zf(z), [f(z)]^2\}\mathrm{d}z\,, \quad i,j\\&= 1,2,6,\end{aligned} \tag{23}$$

$$A^s_{44} = \int_{-\frac{h}{2}}^{\frac{h}{2}} Q_{44}[g(z)]^2\mathrm{d}z, \quad A^s_{55} = \int_{-\frac{h}{2}}^{\frac{h}{2}} Q_{55}[g(z)]^2\mathrm{d}z\,.$$

In this contribution, we use Hamilton's principle to obtain the equations of motion. This principle can be given in analytical form as follows

$$\int_0^t (\delta U - \delta K)\,\mathrm{d}t = 0, \tag{24}$$

where δU represents the change in strain energy; while δK represents the change in kinetic energy.

$$\begin{aligned}\delta U = \int_V \big[&\sigma_x\delta\varepsilon_x + \sigma_y\delta\varepsilon_y + \sigma_{xy}\delta\varepsilon_{xy} + \tau_{xz}\delta\gamma_{xz}\\&+ \tau_{yz}\delta\gamma_{yz}\big]\mathrm{d}V\end{aligned}$$

$$\begin{aligned}\delta U = \int_A \big[&N_x\delta\varepsilon^0_x + N_y\delta\varepsilon^0_y + N_{xy}\delta\varepsilon^0_{xy} + M^b_x\delta k^b_x\\&+ M^b_y\delta k^b_y + M^b_{xy}\delta k^b_{xy} + M^s_x\delta k^s_x\\&+ M^s_y\delta k^s_y\\&+M^s_{xy}\delta k^s_{xy} + S^s_{xz}\delta\gamma^s_{xz} + S^s_{yz}\delta\gamma^s_{yz}\big]\mathrm{d}A.\end{aligned} \tag{25}$$

The change in kinetic energy can be given as

$$\delta K = \int_V [\dot{u}\delta\dot{u} + \dot{v}\delta\dot{v} + \dot{w}\delta\dot{w}]\rho(z)\mathrm{d}V$$

$$\begin{aligned}\delta K = \int_A \Big\{&I_0(\dot{u}_0\delta\dot{u}_0 + \dot{v}_0\delta\dot{v}_0 + \dot{w}_0\delta\dot{w}_0)\\&- I_1\left(\dot{u}_0\frac{\partial\delta\dot{w}_0}{\partial x} + \frac{\partial\dot{w}_0}{\partial x}\delta\dot{u}_0 + \dot{v}_0\frac{\partial\delta\dot{w}_0}{\partial y}\right.\\&\left.+ \frac{\partial\dot{w}_0}{\partial y}\delta\dot{v}_0\right)\\&+J_1\left[(S_1A')\left(\dot{u}_0\frac{\partial\delta\dot{\theta}}{\partial x} + \frac{\partial\dot{\theta}}{\partial x}\delta\dot{u}_0\right)\right.\\&\left.+ (S_2B')\left(\dot{v}_0\frac{\partial\delta\dot{\theta}}{\partial y} + \frac{\partial\dot{\theta}}{\partial y}\delta\dot{v}_0\right)\right]\\&+ I_2\left(\frac{\partial\delta\dot{w}_0}{\partial x}\frac{\partial\dot{w}_0}{\partial x} + \frac{\partial\delta\dot{w}_0}{\partial y}\frac{\partial\dot{w}_0}{\partial y}\right)\\&-J_2\left[(S_1A')\left(\frac{\partial\dot{w}_0}{\partial x}\frac{\partial\delta\dot{\theta}}{\partial x} + \frac{\partial\dot{\theta}}{\partial x}\frac{\partial\delta\dot{w}_0}{\partial x}\right)\right.\\&\left.+ (S_2B')\left(\frac{\partial\dot{w}_0}{\partial y}\frac{\partial\delta\dot{\theta}}{\partial y} + \frac{\partial\dot{\theta}}{\partial y}\frac{\partial\delta\dot{w}_0}{\partial y}\right)\right]\\&+J_3\left[(S_1A')^2\left(\frac{\partial\delta\dot{\theta}}{\partial x}\frac{\partial\dot{\theta}}{\partial x}\right) + (S_2B')^2\left(\frac{\partial\delta\dot{\theta}}{\partial y}\frac{\partial\dot{\theta}}{\partial y}\right)\right]\Big\}\mathrm{d}A,\end{aligned} \tag{26}$$

where dot-superscript convention indicates the differentiation with respect to the time variable t, $\rho(z)$ is the mass density; and (I, J) are the mass inertias defined by

$$\begin{aligned}(I_0, I_1, I_1) &= \int_{-\frac{h}{2}}^{\frac{h}{2}} (1, z, z^2)\rho(z)\mathrm{d}z,\\(J_1, J_2, J_3) &= \int_{-\frac{h}{2}}^{\frac{h}{2}} (f(z), zf(z), f(z)^2)\rho(z)\mathrm{d}z\,.\end{aligned} \tag{27}$$

By replacing the expressions the δU and δK in Eq.(24) and we integrate by parts and separately isolate the coefficients u_0, v_0, w_0, and θ, we obtain the equilibrium equations as follows

$$\begin{aligned}&\delta u_0\colon \frac{\partial N_x}{\partial x} + \frac{\partial N_{xy}}{\partial y} = I_0\ddot{u}_0 - I_1\frac{\partial\ddot{w}_0}{\partial x} + S_1A'J_1\frac{\partial\ddot{\theta}}{\partial x},\\&\delta v_0\colon \frac{\partial N_{xy}}{\partial x} + \frac{\partial N_y}{\partial y} = I_0\ddot{v}_0 - I_1\frac{\partial\ddot{w}_0}{\partial y} + S_2B'J_1\frac{\partial\ddot{\theta}}{\partial y},\\&\delta w_0\colon \frac{\partial^2 M^b_x}{\partial x^2} + 2\frac{\partial^2 M^b_{xy}}{\partial x\partial y} + \frac{\partial^2 M^b_y}{\partial y^2} = I_0\ddot{w}_0 + I_1\left(\frac{\partial\ddot{u}_0}{\partial x} + \right.\\&\left.\frac{\partial\ddot{v}_0}{\partial y}\right) - I_2\left(\frac{\partial^2\ddot{w}_0}{\partial x^2} + \frac{\partial^2\ddot{w}_0}{\partial y^2}\right) + J_2\left((S_1A')\frac{\partial^2\ddot{\theta}}{\partial x^2} + \right.\\&\left.(S_2B')\frac{\partial^2\ddot{\theta}}{\partial y^2}\right),\\&\delta\theta\colon -S_1M^s_x - S_2M^s_y - (S_1A' + S_2B')\frac{\partial^2 M^s_{xy}}{\partial x\partial y} +\\&S_1A'\frac{\partial S^s_{xz}}{\partial x} + S_2B'\frac{\partial S^s_{yz}}{\partial y} = -J_1\left((S_1A')\frac{\partial\ddot{u}_0}{\partial x} + (S_2B')\frac{\partial\ddot{v}_0}{\partial y}\right),\\&+J_2\left((S_1A')\frac{\partial^2\ddot{w}_0}{\partial x^2} + (S_2B')\frac{\partial^2\ddot{w}_0}{\partial y^2}\right)\\&- J_3\left((S_1A')^2\frac{\partial^2\ddot{\theta}}{\partial x^2} + (S_2B')^2\frac{\partial^2\ddot{\theta}}{\partial y^2}\right).\end{aligned} \tag{28}$$

We assume solutions for u_0, v_0, w_0 and θ representing waves propagating in the x-y plane with the form

$$\begin{Bmatrix}u_0(x,y,t)\\v_0(x,y,t)\\w_0(x,y,t)\\\theta(x,y,t)\end{Bmatrix} = \begin{Bmatrix}U\,exp[i(k_1x + k_2y - \omega t)]\\V\,exp[i(k_1x + k_2y - \omega t)]\\Wexp[i(k_1x + k_2y - \omega t)]\\Xexp[i(k_1x + k_2y - \omega t)]\end{Bmatrix}, \tag{29}$$

where U, V, W, and X are the coefficients of the amplitude of the wave, k_1 and k_2 are the wavenumbers of wave propagation along the x-axis and y-axis directions respectively, ω is the frequency. Substitute Eq. (29) in Eq. (28), we obtain

$$([K] - \omega^2[M])\{\Delta\} = \{0\}, \tag{30}$$

Where

$$\{\Delta\} = \{U, V, W, X\}^t. \tag{31}$$

We can write Eq. (30) in matrix form as

$$\left(\begin{bmatrix} S_{11} & S_{12} & S_{13} \\ S_{21} & S_{22} & S_{23} \\ S_{31} & S_{32} & S_{33} \\ S_{41} & S_{42} & S_{43} \end{bmatrix} - \omega^2 \begin{bmatrix} m_{11} & m_{12} & m_{13} \\ m_{21} & m_{22} & m_{23} \\ m_{31} & m_{32} & m_{33} \\ m_{41} & m_{42} & m_{43} \end{bmatrix} \right) \begin{Bmatrix} U \\ V \\ W \\ X \end{Bmatrix} = \begin{Bmatrix} 0 \\ 0 \\ 0 \\ 0 \end{Bmatrix}. \tag{32}$$

The relations of dispersion wave propagation in the FGM plate are written as follows

$$|[K] - \omega^2[M]| = \{0\}. \tag{33}$$

Assuming, $k_1 = k_2 = k$, the roots of Eq. (33) can be given as follows

$$\omega_1 = W_1(k), \omega_2 = W_2(k), \quad \omega_3 = W_3(k), \omega_3 = W_4(k). \tag{34}$$

They correspond to the wave modes M_0, M_1, M_2, and M_3, respectively. The M_0 and M_3 wave modes correspond to the bending wave, the M_1 and M_2 wave modes correspond to the extension wave. The wave propagation phase velocity in the FGM plate can be expressed by

$$C_i = \frac{W_i(k)}{k}, \qquad i = 1,2,3,4 \tag{35}$$

3. Numerical results

3.1 Comparative studies

For the validation and verification of the developed method, comparisons were made with other results already published by other authors. Using Navier's analytical method, to determine eigenvalues of isotropic plates and FGM plates consisting of a mixture of Si3N4 and SUS304. Firstly, we analyze an isotropic plate simply supported with characteristics ($h = 2$ mm, wave number, $k_x = k_y = k$, $\rho = 7480\,\text{kg/m}^3$. The results obtained by the present theory are compared to data available in the literature on the closed-form solution published by Nami and Janghorban (2014) based on the classical theory of plates (CPT) and Aminipour *et al.* (2018) based on higher-order shear strain theory (HOSST). The comparisons agree well with those obtained by CPT and HOSST. Also, physically transverse shear effects always affect the plate behavior.

In the second example, the analysis relates to the case of FGM plates simply supported with a chosen thickness equal to 0.02 m. The mechanical characteristics of the materials used, such as Young's modulus E, density ρ, Poisson's ratio ν, thermal expansion α, and thermal conductivity λ are given in Table 2, which are taken from references (Shen *et al.* 2009, Bui *et al.* 2016). The comparison and validation of this model present a displacement field incorporating indeterminate integral terms with another shear strain approach available in the literature obtained by Sun and Luo (2011) using Reddy's theory. The dispersion curves of the first four wave modes are shown in the Figs. 1 and 2 for the power-law index N equal 0 and 2 respectively. The chosen temperature is the ambient temperature $T_b = T_t = 300$ K.

Table 1 Comparison of the results of frequency mode (M_1). Case of isotropic square plate simply supported

Theory	k				
	5	10	15	20	25
HOSST[a]	160.336	641.28	1442.61	2564.00	4004.96
CPT[b]	160.342	641.37	1443.08	2565.47	4008.55
Present	160.24	639.76	1434.99	2540.17	3947.59

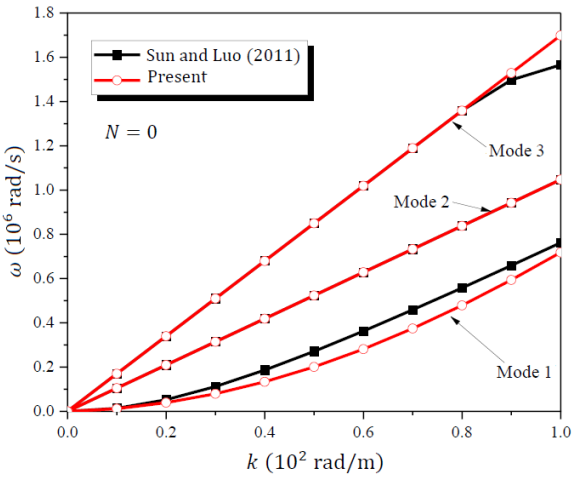

Fig. 1 Comparison of dispersion curves of first three wave modes under thermal environmental conditions $T_b = T_t = 300$ K with $N = 0$

From Figs. 1 and 2 we observe that the present results are in good agreement with those of Sun and Luo (2011) for the two values of the power index $N = 0$ and $N = 2$. However, the proposed model introduces the terms of an indeterminate integral in the displacement field to get only four unknowns. In addition, for instance, for a given value of power-law exponent (i.e., $N = 0$) the difference between the dispersion curves predicted by a new model based on a high-order theory field of displacement is included by introducing indeterminate integral variables and inverse co-tangential function and higher-order shear deformation plate theory obtained by Sun and Lou (2011) for mode 1 and mode 3 in the FGM plate (i.e., $N = 2$).

In the third comparison wave propagation in the FG plate made of a mixture of silicon nitride (Si3N4) ceramic and stainless steel (SUS304) metal are the materials of the upper and lower surfaces of the FGM plate, respectively. The properties of the ceramic and the metal are given in Table 2. The results obtained are illustrated in Table 3. This comparison is also carried out with the results of Sun and Luo (2011) and the results of Aminipour et al. (2018) under thermal environmental conditions $T_b = T_t = 300$ K. We notice that the results obtained by Sun and Luo (2011) and Aminipour *et al.* (2018) and the present theory are in great agreement for distinct volume fraction indices.

Table 2 Physical and mechanical properties of the materials analyzed

Materials	Proprieties	P_{-1}	P_0	P_1	P_2	P_3
Si3N4	E (Pa)	0	348.43 e^{+9}	-3.070 e^{-4}	2.160 e^{-7}	-8.946 e^{-11}
	ν	0	0.2400	0	0	0
	ρ (kg/m^3)	0	2370	0	0	0
	α (1/K)	0	5.8723 e^{-6}	9.095 e^{-4}	0	0
SUS304	E (Pa)	0	201.04 e^{+9}	3.079 e^{-4}	-6.534e^{-7}	0
	ν	0	0.3262	-2.002 e^{-4}	3.797e^{-7}	0
	ρ (kg/m^3)	0	8166	0	0	0
	α (1/K)	0	12.330 e^{-6}	8.086 e^{-4}	0	0

Table 3 Comparison of the results of the mode frequencies. Case of a simply-supported FGM plate, material Si3N4/SUS304 in thermal environmental conditions $T_b = T_t = 300$ K (Sun and Luo 2011)

Theory	*N=0.5*			*N=1*		
	k =80	k = 90	k =100	k =80	k =90	k =100
Aminipour *et al.* (2018)	388.6075	459.8357	532.3897	339.9935	402.1894	465.5563
Sun and Lou (2011)	384.1406	453.6233	524.0754	335.8684	396.4238	457.8079
Present	332.7490	412.3141	498.3111	292.5817	362.6905	438.5160

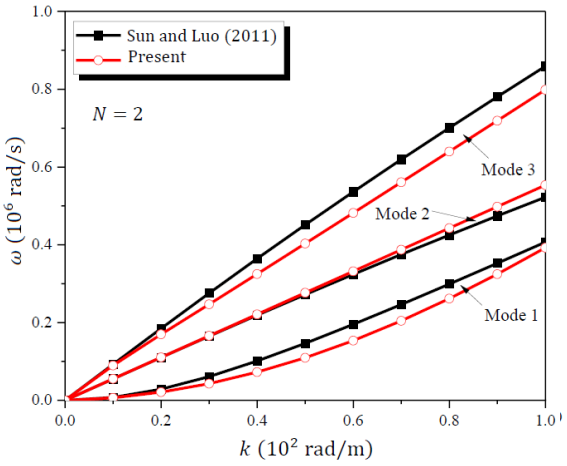

Fig. 2 Comparison of dispersion curves of first three wave modes under thermal environmental conditions $T_b = T_t = 300$ K with $N = 2$

3.2 Parametric study

The dispersion variations for the different wave modes (M_0, M_1, M_2, and M_3) of the functionally graduated plate under thermal environment condition $T_b = T_t = 300$ K are shown in Fig. 3. Different values of the power-law index N were chosen ($N = 0$, 0.5, 1, and 2). It can be observed that the variation in the dispersion curves of the FGM plates is greatly influenced by the volume fraction distributions. In addition, the frequency of wave propagation in the FGM plate decreases as the index of the volume fraction N increases. It is also observed, that the frequency of wave propagation in the homogeneous plate ($N = 0$) is higher compared to those of all cases of FGM plates. Physically, this is because for FG plates, when the volume fraction index is increased, the contained quantity of ceramic increases.

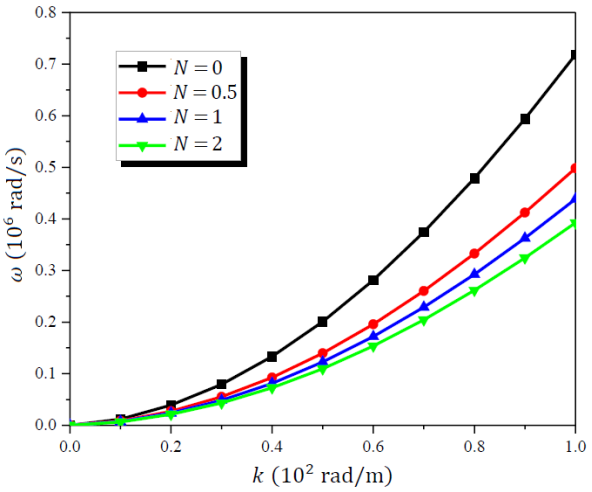

(a) M_0

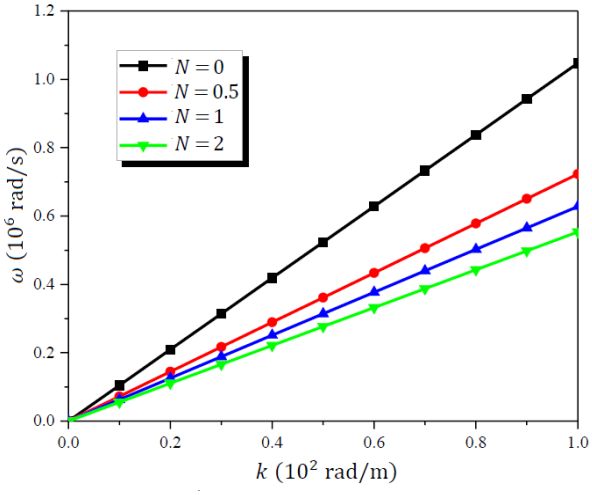

(b) M_1

Fig. 3 The dispersion curves of the different FG plates with ($T_b = T_t = 300$ K)

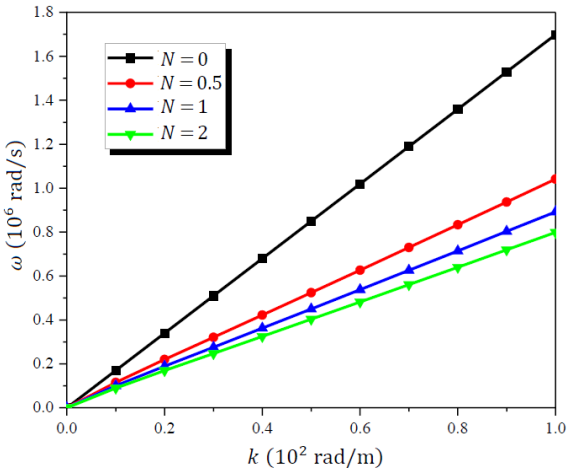

(c) M_2

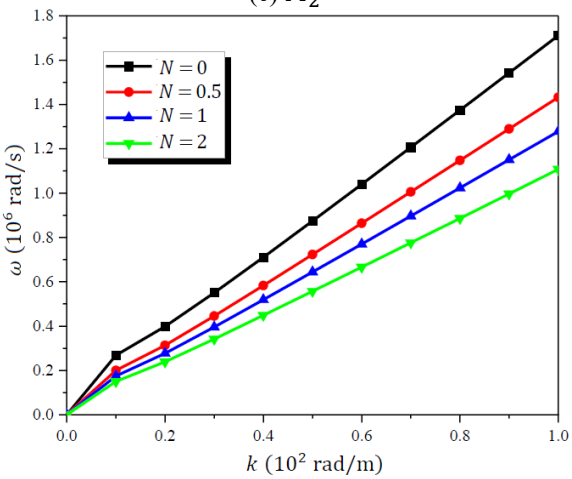

(d) M_3

Fig. 3 Continued-

The phase velocity variations of FGM plates under the condition of the thermal environment $T_b = T_t = 300$ K are shown in Fig. 4. It can be seen that when the index of the volume fraction increases N the phase velocity of the wave propagation in the functionally graded plate decreases for the same value of k. The phase velocity for M_2 and M_3 modes of the isotropic plate ($N = 0$) is a constant, but it is not a constant for the FGM plate ($N \neq 0$). The velocity of the phase of wave propagation in the homogeneous isotropic plate ($N = 0$) is the maximum among those of all functionally graded plates. So, it is clear that the heterogeneity of functionally graded materials has a great effect on the velocity of the wave propagation phase in the FGM plate. In terms of material, nowadays, there is a high demand for high structural implementation and multifunctionality with great mechanical properties (Yang *et al.* 2014a, b, 2015, Kar *et al.* 2015, 2017, Ebrahimi *et al.* 2019a,b, 2022b,c, Assie *et al.* 2011).

Fig. 5 presents the variations of the dispersion of the square FG plate under three different thermal environment conditions such as; case 1 $T_b = T_t = 300$ K; case 2 $T_b = 300$ K, $T_t = 500$ K and case 3 $T_b = 300$ K, $T_t = 800$ K. This analysis is carried out for a value of the power law $N = 2$. We can see that the frequency of wave propagation

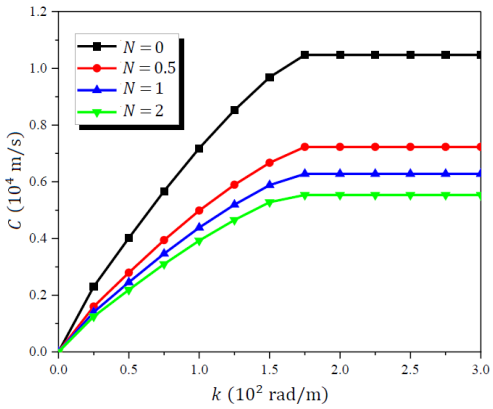

(a) M_0

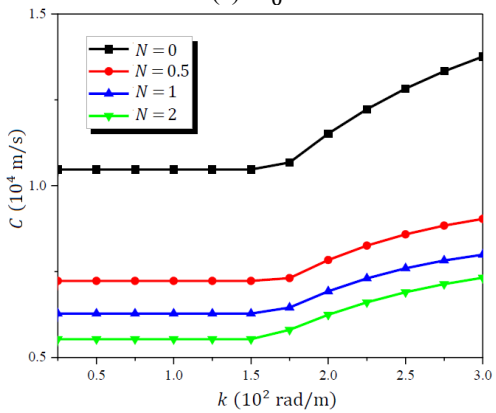

(b) M_1

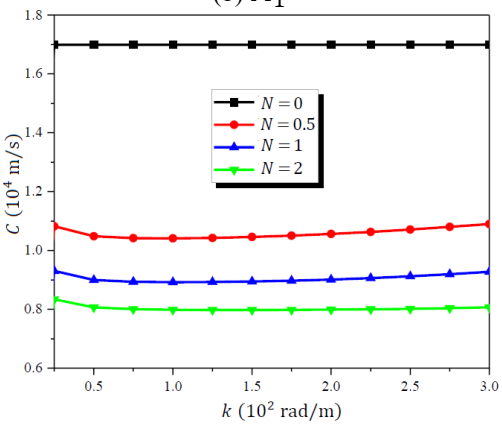

(c) M_2

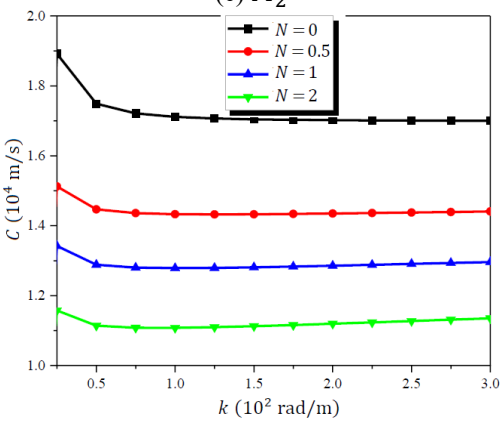

(d) M_3

Fig. 4 The phase velocity curves of the different functionally graded plates ($T_b = T_t = 300$ K)

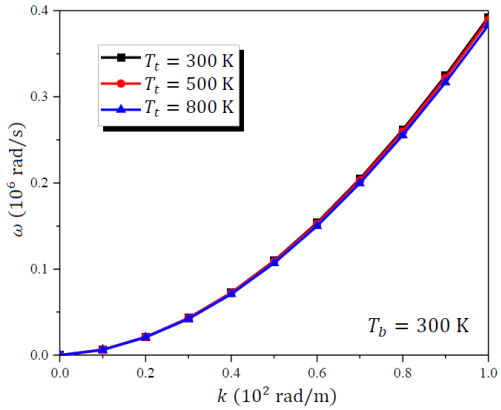

(a) M_0

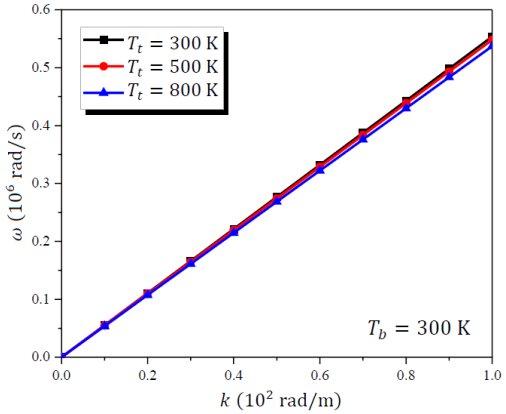

(b) M_1

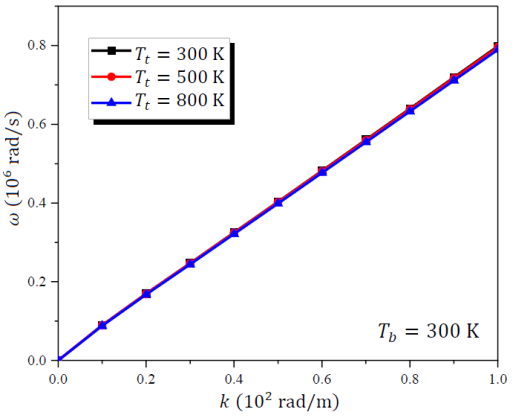

(c) M_2

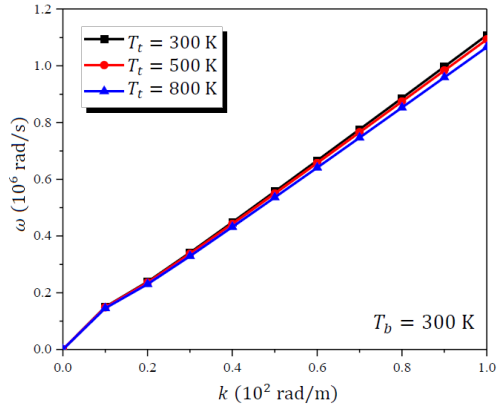

(d) M_3

Fig. 5 The dispersion curves of the FG plate under different thermal environmental conditions with $N = 2$

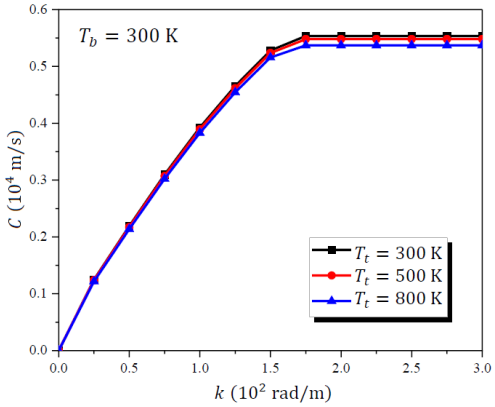

(a) M_0

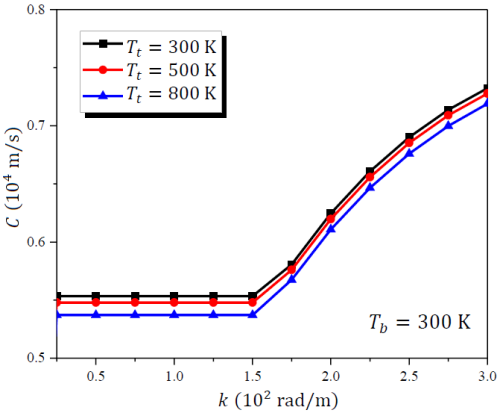

(b) M_1

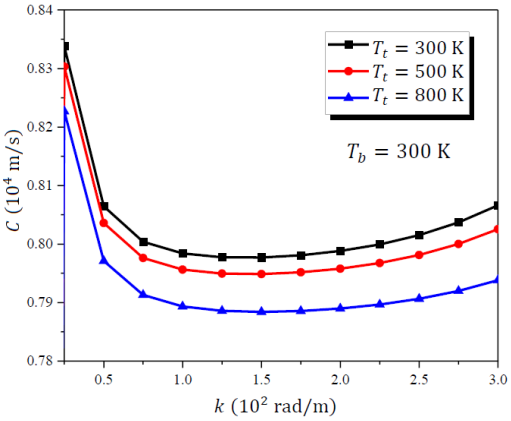

(c) M_2

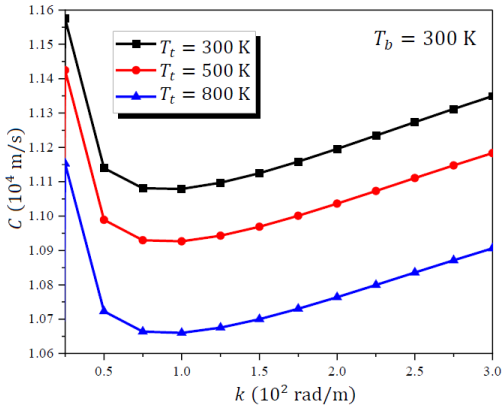

(d) M_3

Fig. 6 The phase velocity curves of the FG plate under different thermal environmental conditions with $N = 2$

in the functionally graded plate decreases with increasing surface temperature differences. We also observe the effect of temperature variation on the frequency of the modes M_0 and M_2 are very small. Fig. 6 shows the phase velocity of the FG plate under different thermal environmental conditions with $N = 2$. It is observed the phase velocity of the FG plate decreases as the surface temperature difference increases.

5. Conclusions

In this contribution, the analysis of wave propagation in functionally graduated plates is examined by a mathematical model that introduces indeterminate integral variables into the displacement field and an inverse cotangential shape function to determine the distribution of deformations and stresses of transverse shears along the thickness. The properties of the materials are assumed to depend on the temperature and to vary in the direction of the thickness according to a simple power-law distribution in terms of the volume fraction of the constituents. The wave propagation equations for the FG plate are obtained by applying the Hamilton principle. The analytical dispersion relation is found by solving an eigenvalue problem. From these results obtained, we can conclude:

- The new class of composite FG materials can be used for different applications, such as thermal barrier coatings for ceramic engines, gas turbines, and optical thin films.
- The accuracy of this approach is determined by comparing its results with other numerical and analytical solutions in the literature. The results of this approach show excellent agreement with the results available in previously published articles.
- The power-law index has a considerable effect on dispersion and phase velocity. On the other hand, the surface temperature it has an also effect on wave propagation and phase velocity.
- The approach presented in this work is simple for the analysis of wave propagation in functionally graduated plates which require only four variables while the theory of higher-order shear strain plates requires five variables.
- Generally, these higher-order shear deformation theories involve higher-order stress resultants that are difficult to interpret physical and require considerably more computational effort.

Finally and through this contribution, we hope to have brought a plus in the analysis of wave propagation in FG plates by a model of four variables that introduce indeterminate integral variables in the displacement field, the present study will be a point useful reference for developing other approaches. In addition, in the future, research is needed on piezoelectric FG structures; carbon nanotube-reinforced composites, and laminated composites with transverse cracks. This contribution deserves to be developed and broadened in new perspectives.

References

Alazwari, M.A., Daikh, A.A. and Eltaher, M.A. (2022), "Novel quasi 3D theory for mechanical responses of FG-CNTs reinforced composite nanoplates", *Adv. Nano Res.,* **12**(2), 117-137. https://doi.org/10.12989/anr.2022.12.2.117.

Aminipoura, H., Janghorbana, M. and Li, L. (2018), "A new model for wave propagation in functionally graded anisotropic doubly-curved shells". *Compos. Struct.* **190**, 91-111.

Ashour, A.S. (2003), "Buckling and vibration of symmetric laminated composite plates with edges elastically restrained", *Steel Compos. Struct*., **3**(6), 439-450. https://doi.org/10.12989/scs.2003.3.6.439.

Assie, A.E., Eltaher, M.A. and Mahmoud, F.F. (2011), "Behavior of a viscoelastic composite plate under transient load", *J. Mech. Sci. Tech.,* **25**, 1129-1140. https://doi.org/10.1007/s12206-011-0302-6.

Basha, M., Daikh, A.A., Melaibari, A., Wagih, A., Othman, R., Almitani, K.H. and Eltaher, M.A. (2022), "Nonlocal strain gradient theory for buckling and bending of FG-GRNC laminated sandwich plates", *Steel Compos. Struct.,* **43**, 639-660. https://doi.org/10.12989/scs.2022.43.5.639.

Becheri, T., Amara, K., Bouazza, M. and Benseddiq, N. (2016), "Buckling of symmetrically laminated plates using nth-order shear deformation theory with curvature effects", *Steel Compos. Struct*., **21**(6) 1347-1368. https://doi.org/10.12989/scs.2016.21.6.1347.

Bensattalah, T., Zidour, M., Daouadji, T.H. and Bouakaz, K. (2019), "Theoretical analysis of chirality and scale effects on critical buckling load of zigzag triple walled carbon nanotubes under axial compression embedded in polymeric matrix", *Struct. Eng. Mech*., **70**(3), 269-277. https://doi.org/10.12989/sem.2019.70.3.269.

Bouazza, M., Antar, K., Amara, K., Benyoucef, S. and Bedia, E. (2019), "Influence of temperature on the beams behavior strengthened by bonded composite plates", *Geomech. Eng*., **18**(5), 555–566. https://doi.org/10.12989gae.2019.18.5.555.

Bouazza, M., Becheri, T., Boucheta, A. and Benseddiq, N. (2019), "Bending behavior of laminated composite plates using the refined four-variable theory and the finite element method", *Earthq. Struct.,* **17**(3), 257-270. https://doi.org/10.12989/eas.2019.17.3.257.

Bouazza, M. and Benseddiq, N. (2015), "Analytical modeling for the thermoelastic buckling behavior of functionally graded rectangular plates using hyperbolic shear deformation theory under thermal loadings". *Multidiscip. Model.Mater. Struct.,* **11**(4), 558-578. https://doi 10.1108/MMMS-02-2015-0008.

Bouazza, M. and Zenkour, A.M. (2020), "Hygro-thermo-mechanical buckling of laminated beam using hyperbolic refined shear deformation theory", *Compos. Struct.,* **252**, 112689. https://doi.org/10.1016/j.compstruct.2020.112689.

Bouderba, B., Houari, M.S.A. and Tounsi, A. (2013), "Thermomechanical bending response of FGM thick plates resting on Winkler–Pasternak elastic foundations", *Steel Compos. Struct.,* **14**(1), 85-104. https://doi.org/10.12989/scs.2013.14.1.085.

Bui, T.Q., Do T.V., Ton, L.H.T., Doan, D.H., Tanaka, S., Pham, D.T., Nguyen-Van T.-A., Yu, T. and Hiros, S. (2016), "On the high-temperature mechanical behaviours analysis of heated functionally graded plates using FEM and a new third-order shear deformation plate theory", *Compos. B Eng.*, **92**, 218-241, https://doi.org/ 10.1016/j.compositesb.2016.02.048.

Bounouara, F., Benrahou, K.H., Belkorissat, I. and Tounsi, A. (2016), "A nonlocal zeroth-order shear deformation theory for free vibration of functionally graded nanoscale plates resting on elastic foundation", *Steel Compos. Struct*., **20**(2), 227-249. https://doi.org/10.12989/scs.2016.20.2.227.

Chen, J., Xu, R., Huang, X. and Ding, H. (2006), "Exact solutions of axisymmetric free vibration of transversely isotropic magnetoelectroelastic laminated circular plates", *Struct. Eng. Mech,* **23**(2), 115-127. https://doi.org/10.12989/sem.2006.23.2.115.

Choudhary, J., Patle, B.K., Ramteke, P.M., Hirwani, C.K., Panda, S.K. and Katariya, P.V. (2022), "Static and dynamic deflection characteristics of cracked porous FG panels", *Int. J. Appl. Mech*., **14**(7), 2250076. https://doi.org/10.1142/S1758825122500764.

Daikh, A.A., Sid Ahmed Houari M. and Eltaher, M.A. (2021), "A novel nonlocal strain gradient quasi-3D bending analysis of sigmoid functionally graded sandwich nanoplates", *Compos. Struct.*, **262**, 113347. https://doi.org/10.1016/j.compstruct.2020.113347.

Dehshahri, K., Nejad, M.Z., Ziaee, S., Niknejad, A. and Hadi, A. (2020), "Free vibrations analysis of arbitrary three-dimensionally FGM nanoplates", *Adv. Nano Res*., **8**(2), 115-134. https://doi.org/10.12989/anr.2020.8.1.013.

Ebrahimi, F., Ghazali, M. and Dabbagh, A. (2022a), "Hygro-thermo-viscoelastic wave propagation analysis of FGM nanoshells via nonlocal strain gradient fractional time-space theory", *Waves Random Complex Media*, In Press. https://doi.org/10.1080/17455030.2022.2105978.

Ebrahimi, F., Seyfi, A., Dabbag, H.A. and Tornabene, F. (2019a), "Wave dispersion characteristics of porous graphene platelet-reinforced composite shells", *Struct. Eng. Mech*., **71**(1), 99-107. https://doi.org/10.12989/sem.2019.71.1.099.

Ellali, M., Amara, K., Bouazza, M. and Bourada, F. (2018), "The buckling of piezoelectric plates on Pasternak elastic foundation using higher-order shear deformation plate theories", *Smart Struct. Syst*., **21**(1), 113-122. https://doi.org/10.12989/sss.2018.21.1.113.

Ebrahimi, F., Ghazali, M. and Dabbagh, A. (2022b), "Hygro-thermo-viscoelastic wave propagation analysis of FGM nanoshells via nonlocal strain gradient fractional time-space theory", *Waves Random Complex Media*, https://doi.org/10.1080/17455030.2022.2105978.

Ebrahimi, F., Khosravi, K. and Dabbagh, A. (2021a), "A novel spatial-temporal nonlocal strain gradient theorem for wave dispersion characteristics of FGM nanoplates", *Waves Random Complex Media*, In press. https://doi.org/10.1080/17455030.2021.1979272.

Ebrahimi, F., Khosravi, K. and Dabbagh, A. (2021b) "Wave dispersion in viscoelastic FG nanobeams via a novel spatial-temporal nonlocal strain gradient framework", *Waves Random Complex Media*, In press. https://doi.org/10.1080/17455030.2021.1970282.

Ebrahimi, F. and Dabbagh, A. (2018), "Effect of humid-thermal environment on wave dispersion characteristics of single-layered graphene sheets", *Appl. Phys. A* **124**, 301. https://doi.org/10.1007/s00339-018-1734-y

Ebrahimi, F., Nouraei, M., Dabbagh, A. and Rabczuk, T. (2019b), "Thermal buckling analysis of embedded graphene-oxide powder-reinforced nanocomposite plates", *Adv. Nano Res*., **7**(5), 293-310. https://doi.org/10.12989/anr.2019.7.5.293.

Ebrahimi, F., Dabbagh, A. and Taheri, M. (2021c), "Vibration analysis of porous metal foam plates rested on viscoelastic substrate", *Eng. Comput*., **37**, 3727-3739. https://doi.org/10.1007/s00366-020-01031-w.

Ebrahimi, F., Nopour, R. and Dabbagh, A. (2022c), "Effect of viscoelastic properties of polymer and wavy shape of the CNTs on the vibrational behaviors of CNT/glass fiber/polymer plates", *Eng. Comput.*, **38**(5), 4113-4126. https://doi.org/10.1007/s00366-021-01387-7.

Ellali, M., Bouazza, M. and Zenkour. A.M. (2022), "Impact of micromechanical approaches on wave propagation of FG plates via indeterminate integral variables with a hyperbolic secant shear model", *Int. J. Comput. Meth*. **19**(9), 2250019. https://doi.org/10.1142/S0219876222500190.

Garg, A., Mukhopadhyay, T., Belarbi, M.O., Chalak, H.D., Singh, A. and Zenkour, A.M. (2023), "On accurately capturing the through-thickness variation of transverse shear and normal stresses for composite beams using FSDT coupled with GPR", *Compos. Struct.*, **305**, 116551. https://doi.org/10.1016/j.compstruct.2022.116551.

Grover, N., Singh, B.N. and Maiti, D.K. (2013), "New nonpolynomial shear-deformation theories for structural behavior of laminated-composite and sandwich plates", *AIAA J*., **51**(8), 1861-1871. https://doi.org/10.2514/1.J052399.

Hissaria, P., Ramteke, P.M., Hirwani, C.K., Mahmoud, S.R., Kumar, E.K. and Panda, S.K. (2022), "Numerical investigation of eigenvalue characteristics (vibration and buckling) of damaged porous bidirectional FG panels", *J. Vib. Eng. Tech*., In press. https://doi.org/10.1007/s42417-022-00677-8

Kahya, V., Karaca, S. and Vo, T.P. (2019), "Shear-deformable finite element for free vibrations of laminated composite beams with arbitrary lay-up", *Steel Compos. Struct*., **33**(4), 473-487. https://doi.org/10.12989/scs.2019.33.4.473.

Kar, V.R., Mahapatra, T.R., Panda. S.K. (2015), "Nonlinear flexural analysis of laminated composite flat panel under hygro-thermo-mechanical loading", *Steel Compos. Struct*., **19**(4), 1011-1033. https://doi.org/10.12989/scs.2015.19.4.1011.

Kar, V.R. and Panda, S.K. (2016), "Nonlinear thermomechanical deformation behaviour of P-FGM shallow spherical shell panel", *Chinese J. Aeronautics*, **29**(1), 173-183. https://doi.org/10.1016/j.cja.2015.12.007.

Kar, V.R. and Panda, S.K. (2017), Postbuckling analysis of shear deformable FG shallow spherical shell panel under nonuniform thermal environment, *J. Therm. Stresses*, **40**(1), 25-39. https://doi.org/10.1080/01495739.2016.1207118.

Mellouli, H., Jrad, H., Wali, M. and Dammak, F. (2019), "Geometrically nonlinear meshfree analysis of 3D-shell structures based on the double directors shell theory with finite rotations", *Steel Compos. Struct*., **31**(4), 397-408. https://doi.org/10.12989/scs.2019.31.4.397.

Nami, M.R. and Janghorban, M. (2014), "Wave propagation in rectangular nanoplates based on strain gradient theory with one gradient parameter with considering initial stress", *Mod. Phys. Lett. B*, **28**(3), 1450021. https://doi.org/10.1142/S0217984914500213.

Nazira, M., Eltaher, M.A., Mohamed, S.A. and Seddek, L.F. (2019), "Energy equivalent model in analysis of postbuckling of imperfect carbon nanotubes resting on nonlinear elastic foundation", *Struct. Eng. Mech*., **70**(6), 737-750. https://doi.org/10.12989/sem.2019.70.6.737.

Pham, Q.H., Tran, T.T., Tran, V.K., Nguyen, P.C., Nguyen-Thoi, T. and Zenkour, A.M. (2022), "Bending and hygro-thermo-mechanical vibration analysis of a functionally graded porous sandwich nanoshell resting on elastic foundation", *Mech. Adv. Mater. Struct.*, **29**(27), 5885-5905. https://doi.org/10.1080/15376494.2021.1968549.

Ramteke, P.M., Kumar, V., Sharma, N. and Panda, S.K. (2022), "Geometrical nonlinear numerical frequency prediction of porous functionally graded shell panel under thermal environment", *Int. J. Nonlinear Mech*., **143**, 104041. https://doi.org/10.1016/j.ijnonlinmec.2022.104041.

Ramteke, P.M., Panda, S.K. and Sharma, N. (2022), Nonlinear vibration analysis of multidirectional porous functionally graded panel under thermal environment", *AIAA J*., In press. https://doi.org/10.2514/1.J061635

Sahoo, B., Sharma, N., Sahoo, B., Ramteke, P.M., Panda, S.K. and Mahmoud, S.R. (2022), "Nonlinear vibration analysis of FGM sandwich structure under thermal loadings", *Structure*s, **44**,

1392-1402. https://doi.org/10.1016/j.istruc.2022.08.081.

Shen, H.S. (2009), Functionally Graded Materials: Nonlinear Analysis of Plates and Shell, CRC Press, https://doi.org/10.1201/ 9781420092578.

Sun, D. and Lou, S.N. (2011), "Wave propagation of functionally graded material plates in thermal environment". *Ultrasonics*, **51**(8), 940-952. https://doi.org/10.1016/j.ultras.2011.05.009.

Tho, N.C., Thom, D.V., Cong, P.H., Zenkour, A.M., Doan, D.H. and Minh, P.V. (2023), "Finite element modeling of the bending and vibration behavior of three-layer composite plates with a crack in the core layer", *Compos. Struct.,* **305**, 116529. https://doi.org/10.1016/j.compstruct.2022.116529.

Yang, Y. and Liu, Y.J. (2020), "A new boundary element method for modeling wave propagation in functionally graded materials", *Europ. J. Mech. – A Solids*, **80**, 103987. https://doi.org/10.1016/j.euromechsol.2019.103897.

Yang, Y., Lam, C.C., Kou, K.P. and Iu, V.P. (2014) "Free vibration analysis of the functionally graded sandwich beams by a meshfree boundary-domain integral equation method", *Compos. Struct.*, **117**, 32-39. https://doi.org/10.1016/j.compstruct.2014.06.016

Yang, Y., Kou, K.P., Iu, V.P., Lam, C.C. and Zhang, C.Z. (2014), "Free vibration analysis of two-dimensional functionally graded structures by a meshfree boundary-domain integral equation method", *Compos. Struct.,* **110**, 342-353. https://doi.org/10.1016/j.compstruct.2013.11.028.

Yang, Y., Kou, K.P., Lam, C.C. and Iu, V.P. (2015) "Free vibration analysis of two-dimensional functionally graded coated and undercoated substrate structures", *Eng. Anal. Bound. Elem*., **60**, 10-17.

https://doi.org/10.1016/j.enganabound.2015.04.009

Zheng, B.J., Yang, Y., Gao, X.W. and Zeng, C.H. (2018), Dynamic fracture analysis of functionally graded materials under thermal shock loading by using the radial integration boundary element method", *Compos. Struct*., **201**, 468-476. https://doi.org/10.1016/j.compstruct.2018.06.050.

Zenkour, A.M. and El-Shahrany, H.D. (2022), "Hygrothermal vibration of a cross-ply composite plate with magnetostrictive layers, viscoelastic faces, and a homogeneous core", *Eng. Comput*., **38**, 4437-4456. https://doi.org/10.1007/s00366-021-01482-9.

CC